Environment. Technology. Resources. Rezekne, Latvia
Proceedings of the 14th International Scientific and Practical Conference. Volume 3, 351-357

Investigating the Impact of Laser Power and Scan Speed on Engraving Aspen Thermowood

Dzintars Rāviņš
Faculty of Engineering
Rezekne Academy of Technologies
Rezekne, Latvia
dzintars.rav@gmail.com

Emil Yankov
Faculty of Engineering
Rezekne Academy of Technologies
Rezekne, Latvia
emol.yankov@rta.lv

Imants Adijans
Faculty of Engineering
Rezekne Academy of Technologies
Rezekne, Latvia
imants.adijans@rta.lv

Lyubomir Lazov
Faculty of Engineering
Rezekne Academy of Technologies
Rezekne, Latvia
lyubomir.lazov@rta.lv

Daivis Rāviņš
Faculty of Engineering
Rezekne Academy of Technologies
Rezekne, Latvia
daivis.rav@gmail.com

Abstract. **This study examines the effect of pre-heat treatment on laser engraving of aspen thermowood. We used an infrared CO_2 laser with a wavelength of 10640 nm to engrave aspen thermowood samples with different pre-treatment temperatures, including one non-treated sample (base). The samples had a similar moisture content of about 8%, but exhibited different shades of brown depending on the pre-treatment temperature. The engraving depth and width were measured for each sample, and 8 graphs were constructed to analyze the results. Our findings show that pre-treatment temperature has a significant effect on the efficiency of laser engraving, with higher pre-treatment temperatures resulting in deeper engraving lines. The study provides valuable insights into the optimization of laser engraving parameters for aspen thermowood, and demonstrates the potential of pre-heat treatment to improve the quality of laser-engraved wooden products.**

Keywords: Aspen thermally modified wood, CO_2 laser engraving, laser processing parameters.

I. INTRODUCTION

The use of laser technology has become increasingly common in various industries since its development in the 1960s. Laser sources are utilized in different technological processes such as marking, engraving, hardening, cladding, cutting, and welding [1], [2], [3]. Lasers have been employed in the wood industry for several decades, primarily for engraving and preparing various design applications in the furniture industry. [4]

Wood is a popular decorative and construction material worldwide. Synthetic wood substitutes cannot compete with natural wood, as it saturates the air with oxygen and has a pleasant aroma. The heat treatment method, based on Finnish pioneers, provides long-lasting protection for wood against the effects of nature, which extends its service life [5].

The laser processing technology is considered one of the most promising methods for engraving. The process of laser processing is complex and depends on three groups of factors: laser source parameters, technological process parameters, and the structure and physical properties of the material being processed [6], [7], [8].

In this method, the material is ablated from the laser impact zone under the influence of the absorbed laser electromagnetic energy. The objective of this study is to investigate the laser ablation process with infrared laser radiation of 10.6 mm wavelength (CO_2 laser) on aspen thermowood samples.

II. MATERIALS AND METHODS

A. Thermally treated wood

This study uses aspen timber that has been processed by drying the wood by heating it to 180 - 230°C. In this process, a comprehensive heat exchanger performance evaluation model and average heat transfer with changes in physical properties can be observed [9], [10]. Wood is

Print ISSN 1691-5402
Online ISSN 2256-070X
https://doi.org/10.17770/etr2023vol3.7250

affected by changes in physical and mechanical properties with moisture content, moisture adsorption, water absorption and volume swelling ratio are reduced, while hygroscopic hysteresis is improved with increasing temperature [11], [12]. Free sugars are carbonized during heat treatment, so it is resistant to rotting, deformation and parasites [13]. Timber quality is directly related to wood moisture content, temperature, and relative humidity control during the drying process. In the process of thermal modification, exposure to high temperatures permanently changes the properties of wood, the most obvious changes and color changes. The wood chosen for processing can be freshly sawn or pre-dried. [14], [15], [16], [17].

The period of thermal treatment of aspen timber takes place with an average time cycle of 36h, as a result of which all the samples used in the experiment are treated uniformly at different temperatures.

Fig. 1. Heat-treated aspen wood samples.

As seen in Fig. 1, heat-treated aspen timber changes tone to a warm brown. The timber is known to start to change tone at roughly 180°C. In this study, six samples of aspen wood were used, including one untreated board and five boards that were heat-treated at temperatures of 180°C, 195°C, 205°C, 214°C, and 225°C, respectively. The moisture content of all samples was determined to be 8% using a digital wood moisture meter HT632. The heat-treatment process used in this study involves a rather complex process of drying the wood, which is important to consider in the analysis of the results.

B. Equipment

For the engraving of the aspen plank samples, a CO_2 laser system (SUNTOP ST-CC9060) with a wavelength of 10640 nm was used (see Fig. 2).

Fig. 2. CO_2 laser system SUNTOP ST-CC9060.

The technical specifications of the SUNTOP ST-CC 9060 laser system are presented in Table 1.

TABLE 1. LASER SYSTEM SUNTOP ST-CC9060 TECHNICAL SPECIFICATIONS

Laser type	CO_2 laser
Operation mode	CW
Wavelength	10640 nm
Maximum output power	100 W
Workspace (Cutting area)	900 x 600 mm
Precision	0,02 mm
Scan speed	0 – 1000 mm/s
Laser Safety Class	4
Cooling system	Water cooling
Data formats used	dxf, plt, bmp, dst,ai
Total power	1500 W

For measuring the depth and width of the engravings, we used a Dino-Lite Edge AM7115MZT digital microscope (shown in Figure 3).

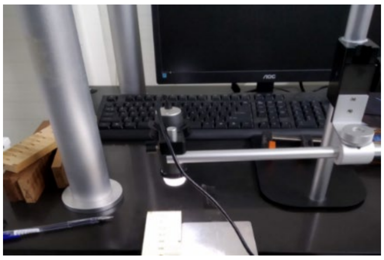

Fig. 3. Dino-Lite Edge AM7115MZT digital microscope.

The specifications of the digital microscope Dino-Lite Edge AM7115MZT are provided in Table 2.

TABLE 2. DINO-LITE EDGE AM7115MZT MICROSCOPE TECHNICAL SPECIFICATIONS

Resolution	2592 × 1944 pixels
Operating System	Windows
Magnification	20x~220x
Unit Dimension	10.5cm (H) x 3.2cm (D)
Lighting	8 white LEDs

METHODOLOGY

In this experiment, six aspen wood samples with dimensions of 13 x 90 x 200 mm were laser engraved using different power densities q_S and scanning speeds v. The power densities used for engraving were 9.3, 2.59, 4.14, 5.39, 6.75, 7.80, and 8.45 ($\times 10^5$) W/cm^2, as listed in Table 4. Each set of parameters was used to engrave five lines, with a distance of 2 mm between each line and a length of 25 mm. The depth h [mm] and width d [mm] of the engraved lines were measured, and graphs were constructed as a function of the laser parameters.

The power output of the laser was measured using an OPHIR F150A-BB-26 laser power meter before starting the experiment. The recorded power values can be found in Table 3.

TABLE 3. AVERAGE POWER DEPENDENCE ON RESONATOR PUMP COEFFICIENT (κP, %)

κP, %	10	15	20	25	30	35	40
***P*, W**	7.3	20.3	32.5	42.3	53.0	61.2	66.3

The power density q_S [W/cm^2] was calculated using formula (1):

$$q = \frac{P}{S} \tag{1}$$

where P [W] is the power and S [cm^2] is the cross-sectional area of the laser beam on the surface of the material to be engraved, as given in formula (2):

$$S = \pi \frac{d^2}{4} \tag{2}$$

with d [cm] being the diameter of the laser beam ($d = 0.01$ cm). The calculated power density values in W/cm^2, corresponding to the measured power values in W (shown in Table 3), are presented in Table 4.

TABLE 4. CALCULATED POWER DENSITY VALUES FOR THE CO_2 LASER SYSTEM

P, W	7.3	20.3	32.5	42.3	53.0	61.2	66.3
$q_S \times 10^5$, W/cm^2	0.93	2.59	4.14	5.39	6.75	7.80	8.45

A matrix of laser technological parameters was generated using the computer program RDWorksV8 (shown in Fig. 4), which supports DXF, AI, and PLT formats and facilitates laser cutting and engraving operations.

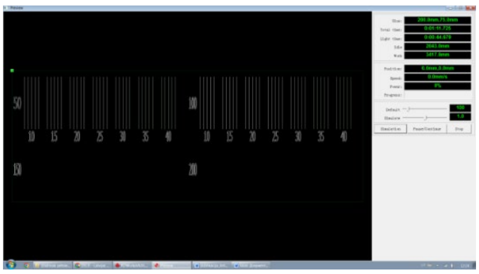

Fig. 4. Matrix of engraving lines in computer program RDWorksV8.

All six aspen wood samples, including one natural aspen wood sample and five aspen thermowood samples, were engraved according to the matrix created in RDWorksV8 (see Fig. 5).

Fig. 5. Photograph of the six aspen wood samples engraved according to the created matrix, including five aspen thermowood samples and one natural aspen wood sample on the right.

To measure the depth of engraved lines, all six aspen wood samples were cut using a circular saw in two pieces through the middle of the engraved lines.

Depth measurement on one of the samples using Dino-Lite Edge AM7115MZT digital microscope is shown in Fig. 6 and width measurement is shown in Fig. 7.

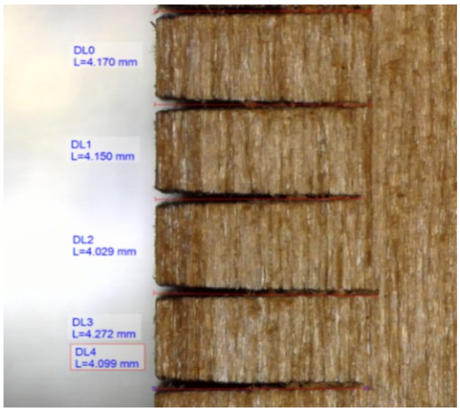

Fig. 6. Measurement of engraving depth on an aspen thermowood sample that was heat-treated at 195°C. (magnification x32).

Fig. 6 shows a heat-treated sample at 195°C with five cuts obtained using a power density $q_S = 8.45 \times 10^5$ W/cm^2 and scan speed v = 50 mm/s. Depth of the cuts are measured and calculated average depth h = 4.14 mm.

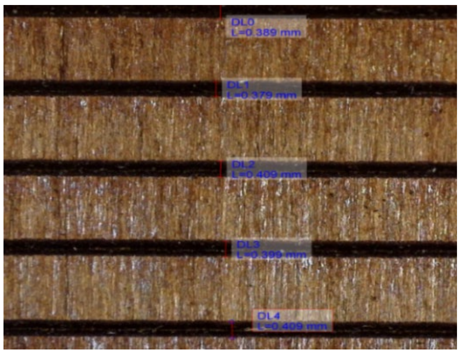

Fig. 7. Line width measurement (magnification x32) - aspen thermowood sample heat-treated at 214°C.

Fig. 7 shows a heat-treated sample at 214°C with five cuts obtained using a power density $q_S = 4.14 \times 105$ W/cm^2

and scan speed v = 100 mm/s. The width of the cuts is measured, and the calculated average width is d = 0.4 mm. The width of engraved lines is measured on the top surface of aspen wood samples, where it is maximum.

III. Results And Discussions

The study results are presented in graphs that depict the impact of laser power density and scan speed on the width and depth of laser engraving lines. The graphs illustrate the relationship between line width and depth as a function of energy density and scanning speed for aspen thermowood samples that have been heat-treated at different temperatures. Specifically, two graphs depict the relationship between line width (d) and power density (q_S) at two scan speeds (50 mm/s and 200 mm/s) for aspen thermowood samples that have been heat-treated at 180°C (Fig. 8) and 225°C (Fig. 9), respectively.

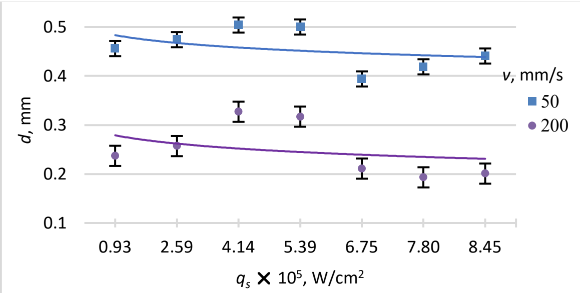

Fig. 8. Dependence of the line width d on the power density q_S at two different scan speed v for aspen thermowood sample heat-treated at 180°C.

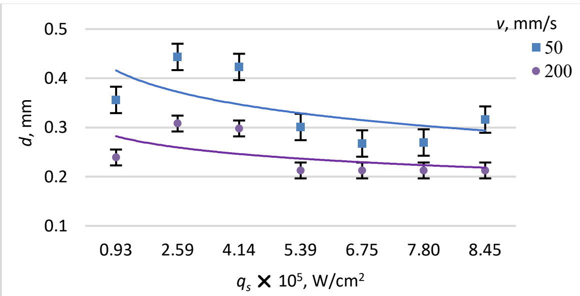

Fig. 9. Dependence of the line width d on the power density q_S at two different scan speed v for aspen thermowood sample heat-treated at 225°C.

The average line width at low scan speed 50 mm/s is 0.46 mm for aspen thermowood heat-treated at 180°C, and 0.34 mm for aspen thermowood heat-treated at 225°C. The average line width at high scan speed 200 mm/s is 0.25 mm for aspen thermowood heat-treated at 180°C, and 0.24 mm for aspen thermowood heat-treated at 225°C. The graphs for these samples are presented in Fig. 8 and Fig. 9, respectively. From these graphs, it can be seen that changes in the line width are small depending on power density, with the width of the lines slightly bigger at lower power density and smaller at higher power density.

Fig. 10 and 11 show the dependence of the line width d on scan speed v at two power density q_S $2.59 \cdot 10^5$ W/cm^2 and $8.45 \cdot 10^5$ W/cm^2 for aspen thermowood sample heat-treated at temperature 180°C (Fig. 10), and aspen thermowood sample heat-treated at temperature 225°C (Fig. 11).

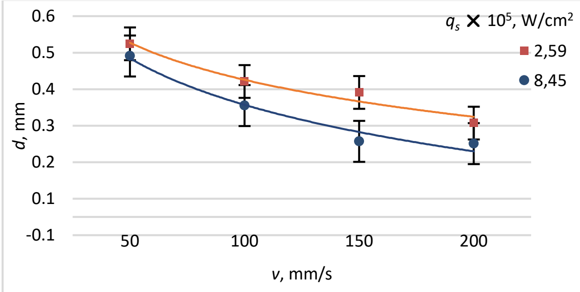

Fig. 10. Dependence of the line width d on scan speed v at two different power density q_S for aspen thermowood sample heat-treated at 180°C.

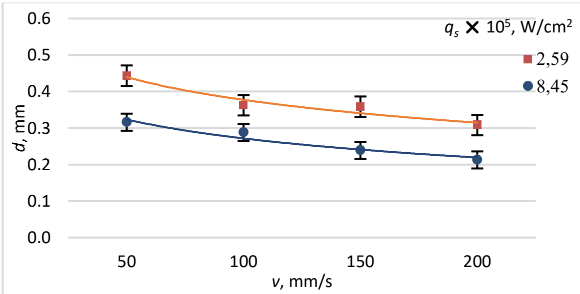

Fig. 11. Dependence of the line width d on scan speed v at two different power density q_S for aspen thermowood sample heat-treated at 225°C.

The line width decreases non-linearly with increasing scanning speed for all engraved samples. The minimum line width is observed at the highest scanning speed of 200 mm/s, reaching a value of 0.2 mm for aspen thermowood samples heat-treated at 180°C. Similarly, the maximum line width is observed at the lowest scanning speed of 50 mm/s, reaching a value of 0.47 mm for the same sample. The trends are similar for the other samples as well.

The rate of width changes tg $d(v)$ [s^{-1}], which depends on the scan speed, is calculated using equation (3).

$$tg\ d(v) = \frac{\Delta d}{\Delta v} \tag{3}$$

where $\Delta d = d_{max} - d_{min}$ is the difference between the maximum and minimum depth, and $\Delta v = v_{max} - v_{min}$ is the difference between the maximum and minimum scan speed. The calculated results of the rate of width changes are shown in Table 5, with units of s-1.

Table 5. The rate of width changes tg $d(v)$ depending on scan speed

tg $d(v)$, s^{-1}	***q_s × 10^5, W/cm^2***	
	2.59	**8.45**
180°C	0.001	0.002
225°C	0.001	0.001

Fig. 12 shows the dependence of the line depth h on power density q_S at two scan speeds v of 50 mm/s and 200 mm/s for the sample of natural aspen.

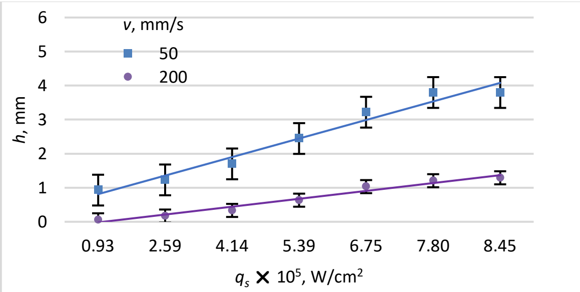

Fig. 12. Dependence of the line depth h on power density q_S at two different scan speed v for the sample of natural aspen.

Fig. 13 shows the dependence of the line depth h on power density q_S at two scan speeds v of 50 mm/s and 200 mm/s for the aspen thermowood sample heat-treated at temperature 225°C.

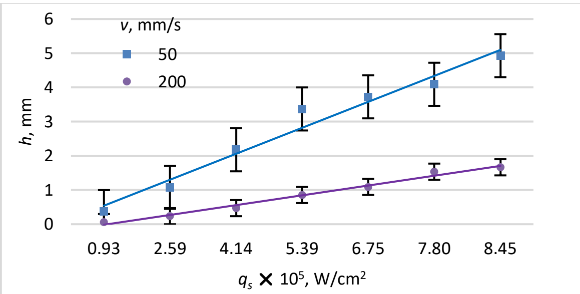

Fig. 13. Dependence of the line depth h on power density q_S at two different scan speed v for aspen thermowood sample heat-treated at 225°C.

The graphs on Fig. 12 and Fig. 13 show that line depth is smaller at low power density and bigger at high power density. The maximum depth of 4.93 mm is reached at power density of 8.45·105 W/cm^2, scan speed 50 mm/s for aspen thermowood sample heat-treated at temperature 225°C, but minimal depth of less than 0.1 mm is reached at power density of 0.93·105 W/cm^2 and scan speed 200 mm/s for both samples. The graphs for the other samples are similar and are in this interval. The increase in line depth is close to linear.

The rate of depth changes tg $h(q_s)$ $[\frac{mm}{W \times cm^2}]$ depending on power density is calculated using equation (4).

$$tg\ h(qs) = \frac{\Delta h}{\Delta qs} \tag{4}$$

Were $\Delta h = h_{\max} - h_{\min}$ is difference between max depth and min depth, and $\Delta q_s = q_{s\ \max} - q_{s\ \min}$ is difference between max power density and min power density. The calculated results of the rate of depth changes are shown in Table 6.

TABLE 6. THE RATE OF DEPTH CHANGES tg $h(q_s)$ DEPENDING ON POWER DENSITY

tg $h(q_S)$, $\frac{mm}{W \times cm^2}$	**v, mm/s**	
	50	**200**
base	0.381	0.164
225°C	0.607	0.213

Two figures below show the dependence of the line depth h on scan speed v at low-power density $q_S = 2.59 \cdot 10^5$ W/cm^2 (see Fig. 14) and high-power density $q_S = 8.45 \cdot 10^5$ W/cm^2 (see Fig. 15) for the sample of natural aspen and aspen thermowood samples heat-treated at temperature 195°C and 225°C.

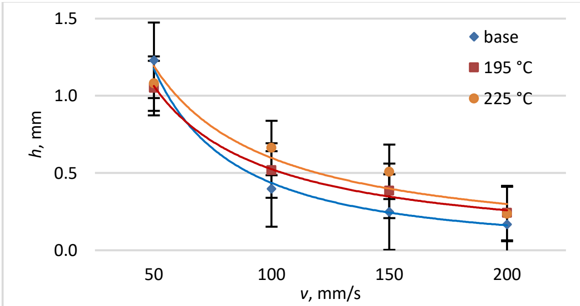

Fig. 14. Dependence of the line depth h on scan speed v at power density $q_S = 2.59 \cdot 10^5$ W/cm^2.

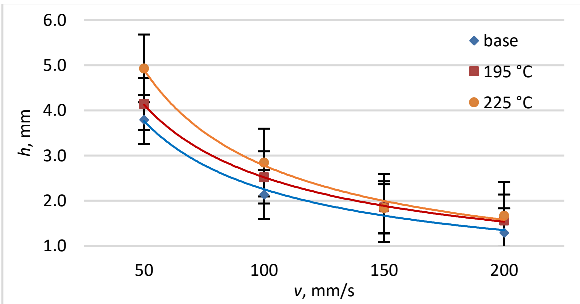

Fig. 15. Dependence of the line depth h on scan speed v at power density $q_S = 8.45 \cdot 10^5$ W/cm^2.

The depth is bigger at low scan speed 50 mm/s, and smaller at high scan speed 200 mm/s. The maximum depth of 4.93 mm is reached at power density $8.45 \cdot 10^5$ W/cm^2 on aspen thermowood sample heat-treated at temperature 225°C, but minimum depth of 0.17 mm at power density $2.59 \cdot 10^5$ W/cm^2 on sample of natural aspen. The decline of the lines on the graphs are non-linear.

The rate of depth changes tg $h(v)$ [s^{-1}] depending on scan speed is calculated using equation (5).

$$tg\ h(v) = \frac{\Delta h}{\Delta v} \tag{5}$$

Where $\Delta h = h_{\max} - h_{\min}$ is the difference between the maximum depth and the minimum depth, and $\Delta v = v_{\max} - v_{\min}$ is the difference between the maximum scan speed and the minimum scan speed. The calculated results of the rate of depth changes are shown in Table 7.

TABLE 7. THE RATE OF DEPTH CHANGES tg $h(v)$ DEPENDING ON SCAN SPEED

tg $h(v)$, s^{-1}	$q_s \times 10^5$, W/cm^2	
	2.59	**8.45**
base	0.007	0.017
195°C	0.005	0.017
225°C	0.006	0.022

Calculation of depth change Δh in percent depending on heat-treated aspen wood obtained using equation (6).

$$\Delta h = \left(\frac{h_{max}}{h_{min}} - 1\right) \times 100\% \quad (6)$$

Table 8 shows calculated depth change in percent for aspen thermowood samples compared to non-treated aspen wood sample. Depth measurements are taken for lines engraved at the max power density q_s = 8.45×10^5 W/cm^2 and min scan speed v = 50 mm/s.

TABLE 8. DEPTH CHANGE Δh IN PERCENT FOR ASPEN THERMOWOOD SAMPLES COMPARED TO NON-TREATED ASPEN SAMPLE AT MAX POWER DENSITY q_S = 8.45 × 10^5 W/cm^2 AND MIN SCAN SPEED V = 50 mm/s

T, °C	h, mm	Δh, %
0	3,80	0,0
180	4,02	6,0
195	4,14	9,2
205	4,20	10,7
214	4,48	18,0
225	4,93	29,8

IV. CONCLUSION

In this study, the laser engraving process was used to investigate the effects of power density and scan speed on the depth of engraved lines on natural aspen wood and aspen thermowood samples. The results showed that the depth of engraved lines is affected by both power density and scan speed, with higher power densities and lower scan speeds leading to deeper lines. Heat treatment of the aspen wood samples also had a significant impact on the depth of the engraved lines, with higher temperatures leading to deeper lines.

The rate of depth changes was calculated for both power density and scan speed, and the results were presented in Tables 6 and 7, respectively. Table 8 showed the depth change in percent for the aspen thermowood samples compared to non-treated samples at the maximum power density and minimum scan speed.

The findings of this study could have important implications for the use of laser engraving in the woodworking industry, particularly in the production of decorative or functional wooden objects. By understanding the factors that affect the depth of engraved lines, manufacturers can optimize their laser engraving processes to achieve the desired results.

Further research could investigate the effects of other laser parameters, such as pulse duration and spot size, on the depth of engraved lines. Additionally, more detailed analyses could be conducted to examine the microstructural changes that occur in the wood during the laser engraving process, as well as the effects of different types of wood on the engraving results.

V. ACKNOWLEDGEMENTS

The authors gratefully acknowledge financial support by the European Regional Development Fund, Postdoctoral research aid Nr. 1.1.1.2/16/I/001 research application "Analysis of the parameters of the process of laser marking of new industrial materials for high-tech applications, Nr. 1.1.1.2/VIAA/3/19/474".

REFERENCES

[1] Lazov L, Angelov N, Teirumnieks E, Teirumnieka E, ''Preliminary Numerical Analysis for the Role of Speed onto Laser Technological Processes'', 2019 Proceedings of the 12th International Scientific and Practical Conf. 3 137-142

[2] Dolchinkov Nikolay T, Lazov L, Ivanov Jordan S, Lilyanova Stelena D, Antons P, ''Use of co2 laser for marking and clearing of textile materials for manufacture of military equipment'', 2019 Proceedings of the 12th International Scientific and Practical Conference. Volume III, 32-36

[3] Artis – Stanislavs Gusts, Imants Adijāns, ''Optimization of parameters for laser marking and engraving on plywood and pine wood materials'' [Online]. Available: https://doi.org/10.17770/het2021.25.6795 [Accessed February 1, 2023].

[4] What is a laser engraving machine for wood, [Online]. Available: https://virmer.com/what-is-a-laser-engraving-machine-for-wood/. [Accessed February 23, 2023].

[5] Andris M, Ilze I, Edgars B, Koksnes ķīmiskā pārstrāde un aizsardzība [Online]. Available: https://www.mf.llu.lv/sites/mf/files/files/lapas/koksnes_parstrade_ieksas_90_gr.pdf. [Accessed February 23, 2023].

[6] Lazov L., N. Angelov, Basic factors determining quality of markings on metals and alloys. International Scientific Conference AMTECH - 2007, Gabrovo, Vol. I, 102-107, 2007

[7] Lazov L., A. Atanasov, N. Angelov, Investigation of the role of certain factors affecting the contrast in laser marking, Contemporary Materials, Vol. II−1, 13-17, 2011.

[8] Shatha M.HasanaKadhim A.HubeatirbDhuha Sh.Abdc , ''Effect of CO_2 laser parameters on redwood engraving process complemented by Taguchi method.'' [Online]. Available: https://doi.org/10.1016/j.matpr.2020.12.580. [Accessed February 25, 2023].

[9] Yanchen Li, Beibei Wang, Weiye,Zhang, Junqi Zhao, Xiaoyang Fang, Jingmeng Sun, Rongqi Xia, Hongwu Guo, Yi Liu, ''Processing wood into a phase change material with high solar-thermal conversion efficiency by introducing stable polyethylene glycol-based energy storage polymer.'' [Online]. Available: https://doi.org/10.1016/j.energy.2022.124206. [Accessed February 2, 2023].

[10] Yuting He, Min Jia, Xiaogang Li, Zhaozhong Yang, Rui Song, ''Performance analysis of coaxial heat exchanger and carrier fluid in medium-deep geothermal energy development'' [Online]. Available: https://doi.org/10.1016/j.renene.2020.12.109. [Accessed February 22, 2023].

[11] Zongying Fu, Yongdong Zhou, Xin Gao, Honghai Liu, Fan Zhou, ''Changes of water related properties in radiata pine wood due to

heat treatment'' [Online]. Available: https://doi.org/10.1016/j.conbuildmat.2019.116692 [Accessed February 22, 2023].

[12] Cristian A.Chávez, Nelson O.Moraga, Carlos H.Salinas, Roberto C.Cabrales, Rubén A.Ananías, ''Modeling unsteady heat and mass transfer with prediction of mechanical stresses in wood drying'', [Online]. Available: https://doi.org/10.1016/j.icheatmasstransfer.2021.105230. [Accessed February 14, 2023].

[13] Shatha M.HasanaKadhim A.HubeatirbDhuha Sh.Abdc , ''Effect of CO_2 laser parameters on redwood engraving process complemented by Taguchi method'' [Online]. Available: https://doi.org/10.1016/j.matpr.2020.12.580. [Accessed February 16, 2023].

[14] Mircea Dulău, Istvan Madaras, ''Development of a Monitoring and Control System for Timber's Drying Process'', [Online]. Available: https://doi.org/10.1016/j.promfg.2019.02.251. [Accessed February 6, 2023].

[15] Published press release "Thermal industry,,, SIA "Ošukalns,, [Online]. Available: https://www.osukalns.lv. [Accessed February 16, 2023], https://www.la.lv/zimols-owood-ar-osukalna-identitati

[16] SIA "Osukalns" internal safety instruction, unpublished documents: Operating_instructions_700764_preliminary

[17] Mircea Dulau, Istvan Madaras, ''Development of a Monitoring and Control System for Timber's Drying Process'' [Online]. Available: https://doi.org/10.1016/j.promfg.2019.02.251. [Accessed February 25, 2023].